

Wavelength Optimization in Spectral Near Infrared Tomography

Matthew E. Eames¹, Brian W. Pogue², and Hamid Dehghani¹

¹ School of Physics, Stocker Road, University of Exeter, United Kingdom,

² Thayer School of Engineering, Dartmouth College, Hanover, NH 03755, USA
m.e.eames@exeter.ac.uk

Abstract: A method is developed to show that instead of using data from the entire spectrum, only selected spectral bands are required to improve image reconstruction accuracy in spectral diffuse optical tomography.

©2007 Optical Society of America

OCIS codes: (100.3190) Inverse problems; (170.3660) Light propagation in tissues;

1. Introduction

Near Infrared (NIR) Diffuse Optical Tomography (DOT) is a non-invasive technique used for obtaining spatial functional images of biological tissue whereby light at wavelengths between 650nm and 930nm is injected into tissue and the emergent light is detected at multiple points on the boundary [1]. This boundary data is then used in a light propagation model to reconstruct chromophore concentrations such as hemoglobin, oxygen saturation, water and scatter properties [2].

There are three main methods used for the collection of NIR data: frequency domain, time domain and continuous wave (CW) systems. Of these CW systems are the simplest to develop and use, however, it has been theoretically shown that absorption and scattering cannot be separated using CW measurements alone without a priori knowledge or the correct choice of multiple wavelengths [3]. Both absorption and scattering in tissue are wavelength dependent, Figure 1, therefore using the correct wavelengths or combination of wavelengths in a spectral model, the chromophore concentrations and scattering properties can be reconstructed directly using spectral image reconstruction techniques [2].

In this work the viability of using large CW data sets containing many wavelengths in the NIR range to achieve a unique solution with minimal crosstalk between chromophores are presented. Other works to date have restricted to finding optimal sets of 5 or 6 wavelengths required for spectral image reconstruction which has shown to reduce the crosstalk between optical parameters [4]. Although a set of 5 or 6 wavelengths will be computationally faster, the use of more wavelengths increases the available information and is therefore important in constraining the inverse problem and hence reducing crosstalk between chromophores. Although not many systems are available that can measure the complete spectrum of transmitted NIR in a tomographic setting, it is important to establish the number and the range of wavelengths used which will ultimately produce functional images of tissue without detriment in its diagnostic accuracy and quality.

2. Methods

Single wavelength reconstruction algorithms cannot distinguish between absorption and scattering using CW data [3]. By using multiple wavelengths in a spectral model this uniqueness problem can be overcome to produce directly images of tissue chromophore concentrations. The choice of wavelengths for the spectral reconstruction is based on two considerations; (1) the absorption parameters must be separable from the scattering parameters and (2) the absorption chromophores must be separable from each other. These criteria have been established and are derived from Beer's law and a non-uniqueness proof for CW data [4]. These conditions provide two parameters that need to be optimized; (a) a residual which must be as large as possible to give a unique solution and (b) a condition number which must be as small as possible so that each chromophore has an equal contribution to the total absorption. Although this method has been formulated such that scattering amplitude can vary, it has been found difficult to reconstruct scatter power reliably using a CW system without additional information about NIR path-length in tissue. In this work, therefore, the assumption is still made that scatter power is known and kept at a constant.

In Figure 1(a) the absorption spectra for 3 chromophores (deoxygenated hemoglobin (Hb), oxygenated hemoglobin (HbO) and water (H₂O)) are shown. The residual and low condition number, as defined above, have been calculated assuming that NIR data are available at either 4, 5 or 6 wavelengths and the repetition of each wavelength appearing at optimal residual and condition numbers have been plotted as a histogram in Figure 1 (b-d). For a data set of 4 wavelengths the most frequent wavelengths which maximize the residual and reduce the

BMD36.pdf

condition number are found in the ranges 650nm to 660nm, 708nm to 744nm, 772nm to 930nm. Increasing the number of wavelengths to 5 and 6 alters the size and position of the spectral bands of significant wavelengths and also increases the magnitude of the normalized counts for each window. For 6 wavelength sets, the second spectral band from the 4 wavelengths sets becomes wider (680nm to 750nm) and the third spectral band splits into two separate bands to between 802nm and 886nm and a single peak at 930nm.

For the 6 wavelength set the peak at 650nm clearly corresponds to the peak in the absorption due to deoxygenated hemoglobin while the peak at 930nm corresponds to the peak in the absorption due to water. The flat band of wavelengths between 802nm and 886nm corresponds to a low peak in oxygenated hemoglobin. The large peak from 680nm and 750nm is positioned around the intersection points of all 3 chromophores.

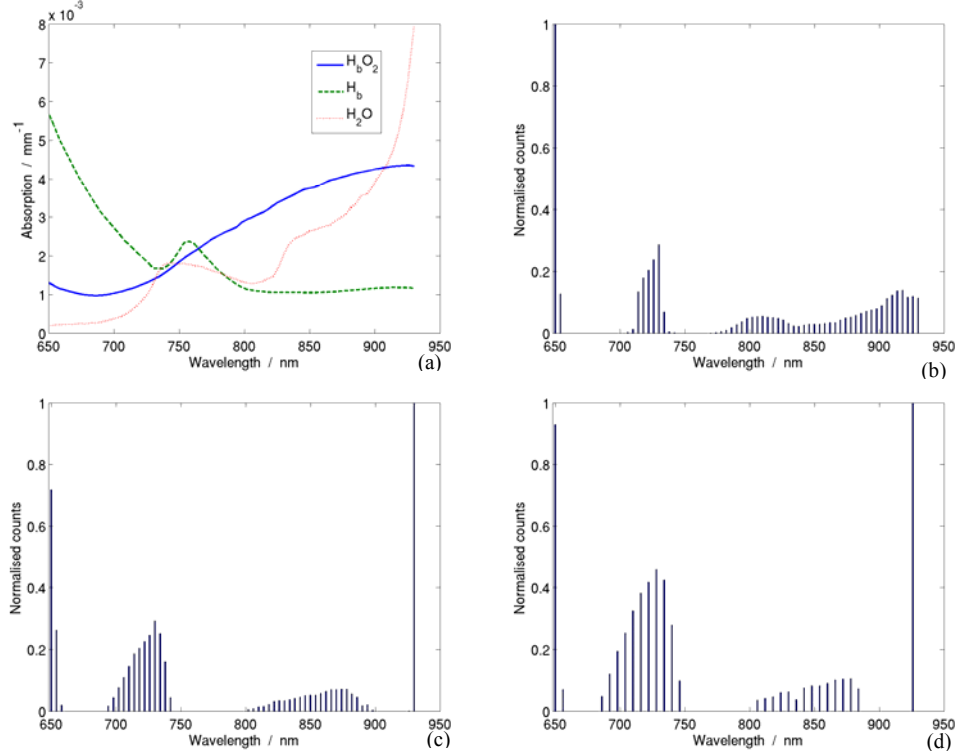


Figure 1. (a) Absorption spectra for oxygenated hemoglobin, deoxygenated hemoglobin and water and normalized counts for most frequent wavelengths with high residual and low condition for (b) 4 wavelengths, (c) 5 wavelengths and (d) 6 wavelengths.

3. Results

To further investigate the effects of the chosen wavelength sets, images are reconstructed using simulated data with a 2D circular mesh of radius 43mm with 1785 nodes corresponding to 3418 linear elements. The background HbO and Hb concentration is 0.01 μ M, the water content is 40%, the scattering amplitude is 1mm⁻¹ and the scatter power is 1. Four separate heterogeneous anomalies of radius 7.5mm are placed with equal angular distribution around the circular mesh, Figure 2, and for each anomaly only a singular chromophore is changed corresponding to either a HbO concentration of 0.02 μ M, Hb concentration of 0.02 μ M, water content of 80% or scattering amplitude 0.5mm⁻¹. 16 optical fibers are placed on the boundary generating a total of 240 CW measurements per wavelength.

The forward model data is modeled using NIRFAST, a finite element method solution to the diffusion equation. The inverse problem is solved iteratively to find the optical parameters at each node using the Moore-Penrose inverse, $J^T(JJ^T + \lambda I)^{-1} \delta \Phi$, where $\delta \Phi$ is the data vector, $\delta \mu$ is the solution vector for the optical properties and J is the Jacobian matrix. λ is a regularization factor which is scaled by the maximum of the diagonal of JJ^T and reduced at each iteration.

To show the difference between the choice of wavelength sets, images are reconstructed using three different wavelength sets and are displayed in Figure 2; (1) 6 optimal wavelengths from analysis of Figure 1(d): 650, 650nm, 704nm, 722nm, 734nm, 878nm and 930nm. (2) wavelengths at 4nm separation at 4 bands of 650nm to 658nm, 680nm to 750nm, 802nm to 886nm and 930nm and (3) wavelengths at 4nm separation between 650nm and 930nm.

As the number of wavelengths increases the reconstructed values tend towards the true target values and cross talk between chromophores decreases. However very little qualitative and quantitative difference is seen between

BMD36.pdf

using all wavelengths (71 wavelengths) and the selection of wavelengths within the spectral bands of figure 1(d) (44 wavelengths). However the computation time decreases dramatically from 18346 seconds to 7279 seconds when using wavelengths at only the four defined bands.

4. Discussion

In this work it is shown that a large selection of wavelengths can reduce the cross talk between chromophores during image reconstruction and increase the qualitative and quantitative accuracy. By selecting wavelengths which contribute mostly to a large residual and a low condition number, similar results can be achieved to using the entire spectrum improving the computation time considerably while not impinging on the image quality. The results here indicate that using wavelengths at specific bands (windows) within the NIR spectrum, provide as much information to improve the accuracy of spectral imaging, while at the same time dramatically reducing the computation time. Further work will investigate the effect of the assumed scattering power within the image reconstruction, and to investigate the set of wavelengths that would allow the reconstruction of additional chromophores as well as the unknown scattering amplitude and power.

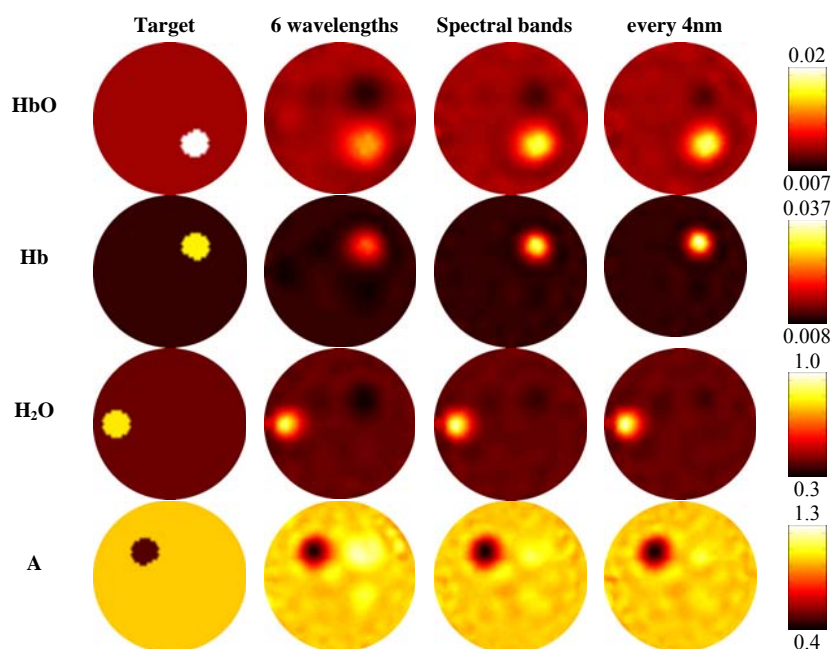


Figure 2. Reconstructed chromophore concentrations for the 3 spectral wavelength choices of 6 wavelengths (650nm, 704nm, 722nm, 734nm, 878nm and 930nm), the spectral band method (650nm to 658nm, 680nm to 750nm, 802nm to 886nm and 930nm) and all wavelengths (650nm and 930nm with a step size of 4nm). In each case the scatter power, b , is constant at 1.

5. Acknowledgements

This work has been sponsored by EPSRC, UK.

6. References

1. Dehghani, H., Pogue, B. W., Poplack, S. P., Paulsen, K. D., *Multiwavelength Three-Dimensional Near-Infrared Tomography of the Breast: Initial Simulation, Phantom, and Clinical Results*. Applied Optics, 2003. **42**(1): p. 135-145.
2. Srinivasan, S., Pogue, B. W., Brooksby, B., Jiang, S., Dehghani, H., Kogel, C., Poplack, S. P., and Paulsen, K. D., *Near-Infrared Characterization of Breast Tumors In Vivo using Spectrally-Constrained Reconstruction*. Technology in Cancer Research & Treatment, 2005. **5**(5): p. 513-526.
3. Arridge, S.R. and W.R.B. Lionheart, *Nonuniqueness in diffusion-based optical tomography*. Optics Letters, 1998. **23**(11): p. 882-884.
4. Corlu, A., Choe, R., Durduran, T., Lee, K., Schweiger, M., Arridge, S. R., Hillman, E. M. C., Yodh, A. G., *Diffuse optical tomography with spectral constraints and wavelength optimization*. Appl. Opt., 2005. **44**(11): p. 2082-2093.